



## HIGH RESOLUTION ELECTRON MICROSCOPY STUDIES IN CARBON SOOTS

M. MIKI-YOSHIDA, R. CASTILLO, S. RAMOS, L. RENDÓN, S. TEHUACANERO,  
B. S. ZOU, and M. JOSÉ-YACAMÁN  
Instituto de Física, UNAM, P.O. Box 20-364, Mexico D.F. 01000, Mexico

(Received 9 June 1993; accepted in revised form 3 August 1993)

**Abstract**—A descriptive study using high resolution electron microscopy of fullerene-related carbon structures found in carbon soots is presented. Nanotubules, onions, small particles, carbon fibers, and tangled structures are some of the structures characterized here. Several methods, such as arc discharge, catalytic induced growth from vapor, heating, and electron irradiation were used to prepare the carbon soot samples. Several structures are reported here, such as tangled balls of graphite, self-arranged ellipsoidal graphite rings, and fiber structures grown from vapor. In the last case, we also show that the shape of the growing fiber layers is determined by the shape of the substrate particles.

**Key Words**—High resolution electron microscope, fullerene, nanotubules, onions.

### 1. INTRODUCTION

The recent discovery of the carbon fullerenes[1,2] has triggered a new exciting field of research, where a great variety of new structures, such as carbon onions[3] and carbon tubes[4], has been produced. Moreover, those kinds of structures are present in other layered materials, such as in  $WS_2$ [5]. Therefore, this has broadened the possibility of finding practical uses for these novel structures in the near future. On the other hand, theoretical calculations have shown that carbon nanotubes can have relevant properties, such as very high capillarity[6], or size-dependent electrical conductivity[7].

In spite of the wide interest in fullerene-related materials, very little is known about the great variety of structures found in carbon soots, the relation between them, or their stability. Moreover, our understanding about the relation between these structures and their kinetics of formation is quite scarce. Therefore, characterization studies are needed, in particular those relating the structures to methods of production.

In this work, we present the first of a series of papers devoted to the characterization with high resolution electron microscopy (HREM) of several structures found in carbon soots. Here, we will present carbon nanotubes, onion-like structures, irregular structures such as tangled balls of graphite, self-arranged ellipsoidal graphite rings, and small particles.

### 2. EXPERIMENTAL

#### 2.1 Carbon Samples

A first set of samples was prepared by the arc-discharge method. We denote these samples as AD samples. Here, the nanotubes were obtained in a

graphite rod contact-arc reaction vessel, similar to the  $C_{60}$  generator of Haufler *et al.*[8]. According to our system design, a 6-mm o.d. graphite rod was kept at a distance of 1–2 mm from a 30-mm o.d. graphite disk by gentle spring pressure. This device was inside a closed cylindrical container of 10 cm o.d., 30 cm long, surrounded with copper tubing for cooled water. The container was also inside a high vacuum chamber, with proper connections to vacuum pumps and to helium supply. Before the arc was generated, the chamber was pumped down to  $10^{-3}$  Pa, and helium was fed to a pressure up to 400 torr. Graphite rod (–negative) and disk (+positive) connections were made with copper clamps connected through vacuum feedthroughs to an external dc high-current power source (Lincoln shield arc welder). The graphite disk was electrically isolated with a teflon disk. In addition, the cylindrical container and the chamber were provided with aligned windows in order to follow the temperature with a pyrometer (2773–3300 K). After the graphite rod was consumed, the deposits on the graphite disc were dispersed in toluene with the aid of an ultrasonic cleaner, and samples from these suspensions were deposited on electron microscope copper grids.

A second set of samples was prepared by heating the carbon soot. The first kind of sample, denoted as HF samples, were obtained by direct heating in a muffle furnace. We started with commercial carbon soot produced by Strem Chemicals (MA). The carbon soot, 3.4 wt% of  $C_{60}$  –  $C_{70}$ , was encapsulated in an evacuated quartz tube at a pressure of  $10^{-3}$  Pa. The temperature was raised from ambient up to 1073 K at a rate of  $0.4 \text{ K s}^{-1}$ , and it was maintained for 180 s. After, the carbon soot was slowly cooled down ( $0.07 \text{ K s}^{-1}$ ) to ambient temperature. A second kind of carbon soot samples were also heated, but in a different way. These were heated in-situ up to

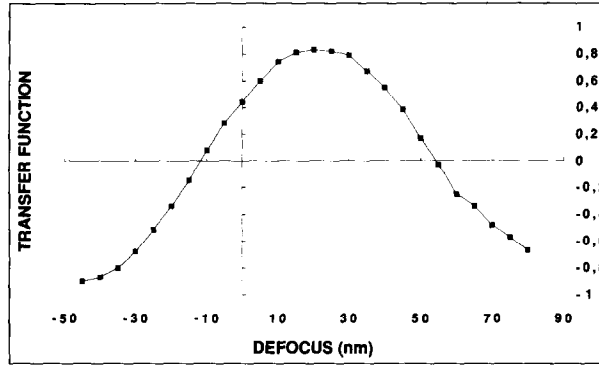


Fig. 1. The contrast transfer function as a function of defocus for the JEOL 4000 EX electron microscope used in this work.

1073 K during several minutes, in a transmission microscope (TEM) with a heating stage. The rates of heating and cooling in this case were  $0.3 \text{ K s}^{-1}$  and  $0.9 \text{ K s}^{-1}$ , respectively. We refer to these samples as HEM samples.

A third set of samples was irradiated with the electron beam from a Van de Graaf electron accelerator (VGEA) or with the electron beam of a TEM. We refer to these samples as IRA and IRM samples, respectively. In the first case, irradiation of carbon soot inside of polyethylene bags was performed in the VGEA with a 1 MeV electron beam. The dose intensity was  $1.7 \times 10^{-2} \text{ Mrad s}^{-1}$ , to complete a total dose of 1000 Mrad. In the second case, the

carbon soot was irradiated in-situ in a TEM. Here the vacuum was better than  $10^{-4} \text{ Pa}$ . The beam intensity was of  $100 \text{ A cm}^{-2}$ .

Soot samples coming from the second and the third sets were suspended in pure ethanol, and drops from these suspensions were deposited on electron microscope grids.

We have produced a final set of samples using catalytic methods[9]; we will denote these as CT samples. Partial results from these studies have been reported elsewhere[9]. This is a very efficient method for producing carbon fibers[10], and we have shown before that carbon nanotubules can be produced by this method too[9].

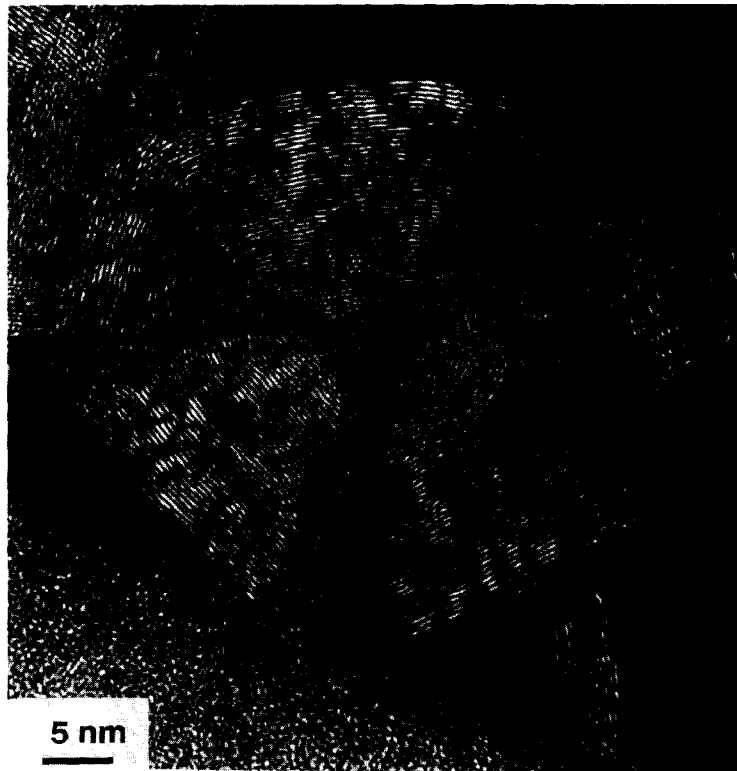


Fig. 2. Structure of a giant fulleroid. This is very similar to that presented by Ugarte[3].

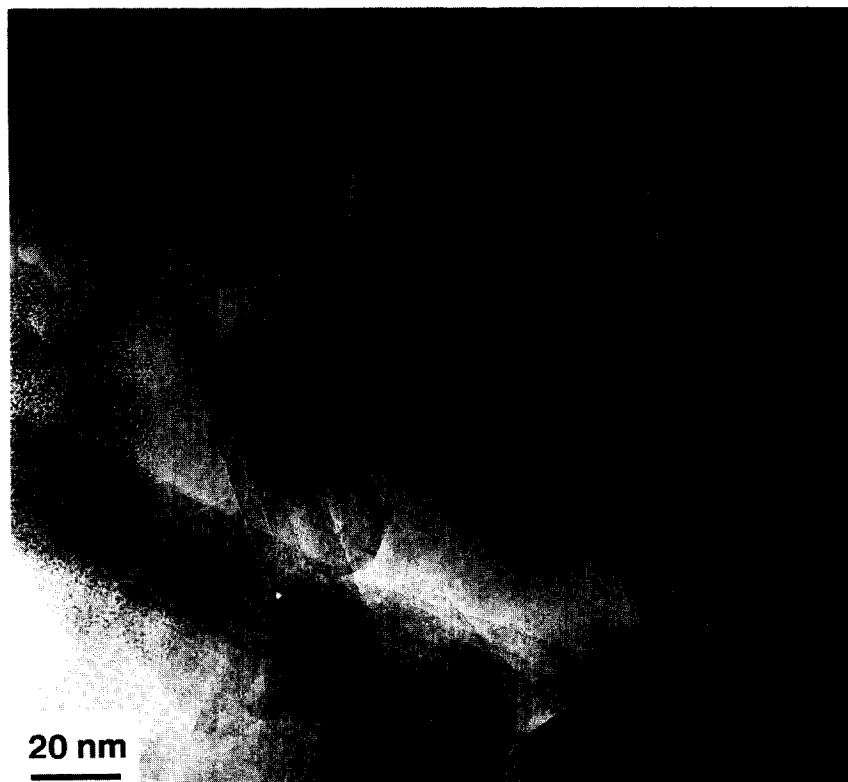


Fig. 3. Region showing different kinds of fulleroid structures, including a faceted hexagonal one.

## 2.2 Electron microscope techniques

A JEOL 4000 EX microscope with a resolution of 1.4 Å was used. The contrast transfer function of the microscope as a function of the defocus of the objective lens is shown in Fig. 1. This transfer function was calculated for the graphite (0001) planes. As can be observed in Fig. 1, a defocus value of 25 nm will allow observation of the graphite (0001) planes as bright lines (separation of  $3.35_4$  Å). Under these conditions, the observation is quite favorable and a maximum of information can be extracted from carbon samples.

Some of the microscope images were computer processed, using a charge-coupled device (CCD) system, to obtain the fast Fourier transform (FFT) of the microscope images. The transformed images were filtered using different masks and back transformed to recover microscope images. Using this method, noise levels of the images can be significantly reduced.

Some samples of the second set (HF and HEM) were also studied with a parallel electron energy loss spectroscopy system (EELS) coupled to the electron microscope. The EELS spectra allows the identification of carbon particles.

Samples of the second and third sets were also studied by selected area electron diffraction (SAED), x-ray diffraction, and proton induced x-ray emission. An extensive study using these techniques was recently presented[11].

## 3. EXPERIMENTAL RESULTS

### 3.1 Onion-like and tubular structures

Onion-like structures were reported earlier by Iijima[12], and recently they were thoroughly studied by Ugarte[3]. These structures correspond to a giant fulleroid structure. Structures of this kind were found in AD samples. An example is shown in Fig. 2. One interesting feature is that, these structures often grow up joined to amorphous carbon (as shown in Fig. 2). In a few cases, onionlike structures nucleated out of the amorphous carbon phase. The inner circles of these carbon structures are not well defined. They are easily deteriorated after a few minutes of observation in a TEM, due to electron beam damage. To obtain the structure presented in Fig. 2, care was taken to prevent damage by electron irradiation.

The fact that onion structures are 3-dimensional can be proven by the dark contrast running along the radius. Moreover, after tilting the sample lattice, resolution does not disappear, confirming the three-dimensional nature of the structure.

The onion structures can have several shapes. An example is shown in Fig. 3 for the case of AD samples. Here, we show a structure with an ellipsoidal shape, a structure with a distorted hexagonal shape, as well as other onions with irregular shapes. These onions tend to be grouped and attached to other kinds of structures on the sample. Moreover,

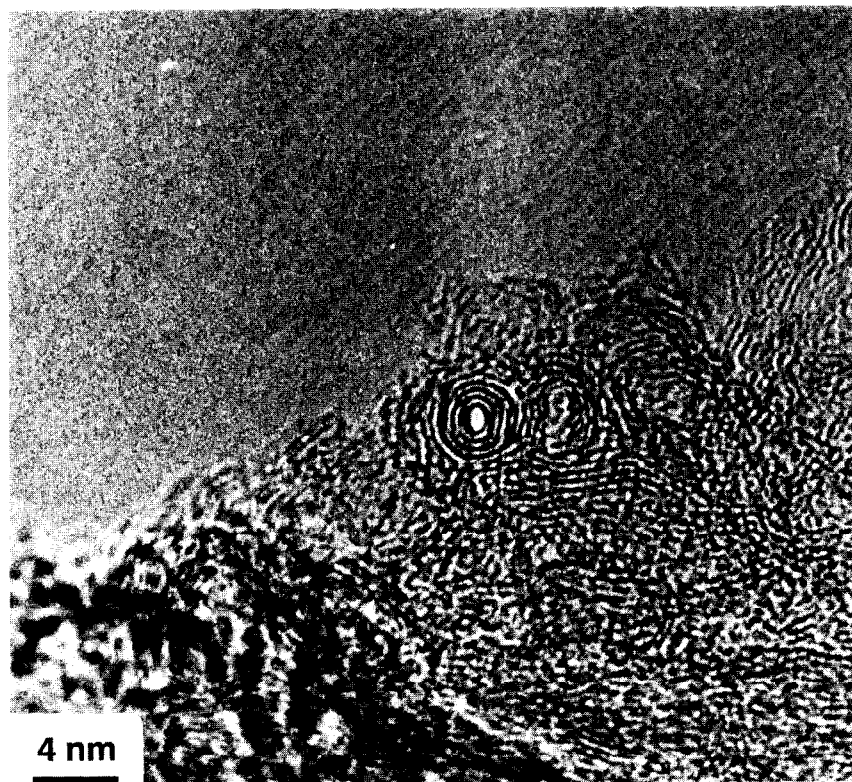


Fig. 4. Very small onion structure with a radius of *ca* 20 Å.

the onion structures tend to grow, on the average, up to a diameter of *ca* 30 nm. However, faceted structures such as the hexagonal ones shown in Fig. 3, can reach up to 60 nm.

HF samples can show very small onion structures such as those shown in Fig. 4. This structure consists of only four layers of graphite. It has a radius of *ca* 2 nm, including the void space in the central part. It should be noted that even at this size level, faceting is quite remarkable. It is important to note, that the onion structure in Fig. 4 was produced in the middle of amorphous materials.

Figure 5 shows an example of a large onion structure (marked with A) that is joined to another large onion structure (marked as B); both of them are joined to a nanotube structure (marked as C). This latter structure is also folded around point C. Figure 5 comes from AD samples. As shown by Iijima[13], to change the direction of growth, pentagonal arrays of carbon atoms (+60° disclination) or a heptagonal ones (-60° disclination) must be introduced in the nanotubes.

### 3.2 Ordered graphite rings and tangled structures

We found that, under some conditions, AC samples allow us to observe the formation of an ordered array of graphene rings such as those shown in the Fig. 6a. Figure 6b is the computer processed image

of Fig. 6a. Here, the frequencies corresponding to background were eliminated. In both figures, most of the rings are composed of a single layer of graphene, and they can be circular or ellipsoidal. We note that in some instances two consecutive rings are connected. However, in most of the cases, each ring remains as an individual object. In this case, the boundary between two rings has the width of (0001) graphite planes, and the mean diameter of the rings is around 2 nm. A remarkable fact is that, the mean distance between circle centers is also around 2.5 nm. This distance is close to that expected for the lattice parameters of schwarzite structures[14]. The rings form approximate hexagonal arrays, and can be ordered in distances up to 50 nm. Also, we have observed arrays of rings that are irregularly stacked, and very large structures (up to 1 μm) can be generated. These samples show many arrays of ring structures, which can be destroyed by the high intensity electron microscope beam. Our results show a new way in which the graphene can be self-arranged in rings structures, with diameters and interring distances of the order of those predicted for carbon structures with negative gaussian curvature[13].

AD samples can also show how the ordered structures of Fig. 6 may become irregular, producing a very complex tangled arrangement of curved graphene sheets as shown in Fig. 7 (region marked with an arrow). This kind of material shows in a

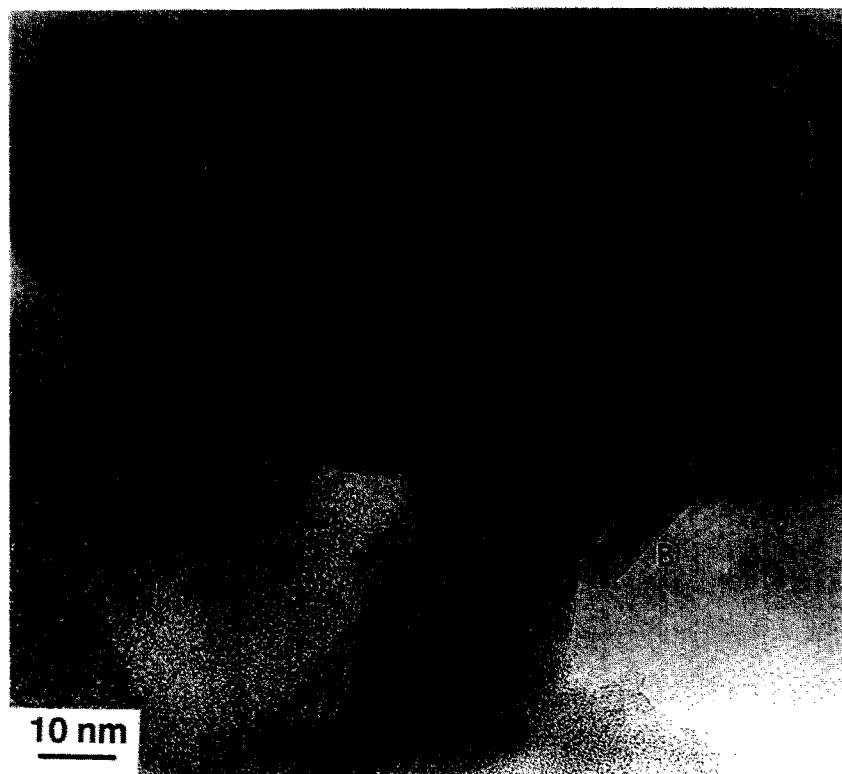


Fig. 5. Onion structures attached to a nanotube. The nanotube is folded around point C.

very remarkable way the flexibility of these graphene sheets. The amorphous nature of these materials seems to arise from the complex folding of the tangled structures. These graphene sheets form ball-like structures that are attached or superimposed to nanotubes or other structures (Fig. 8). These ball structures, shown in Fig. 9, can have a diameter of the order of 40 nm. Tangled forms are very common in AD samples. However, as far as we know, they have not been reported before.

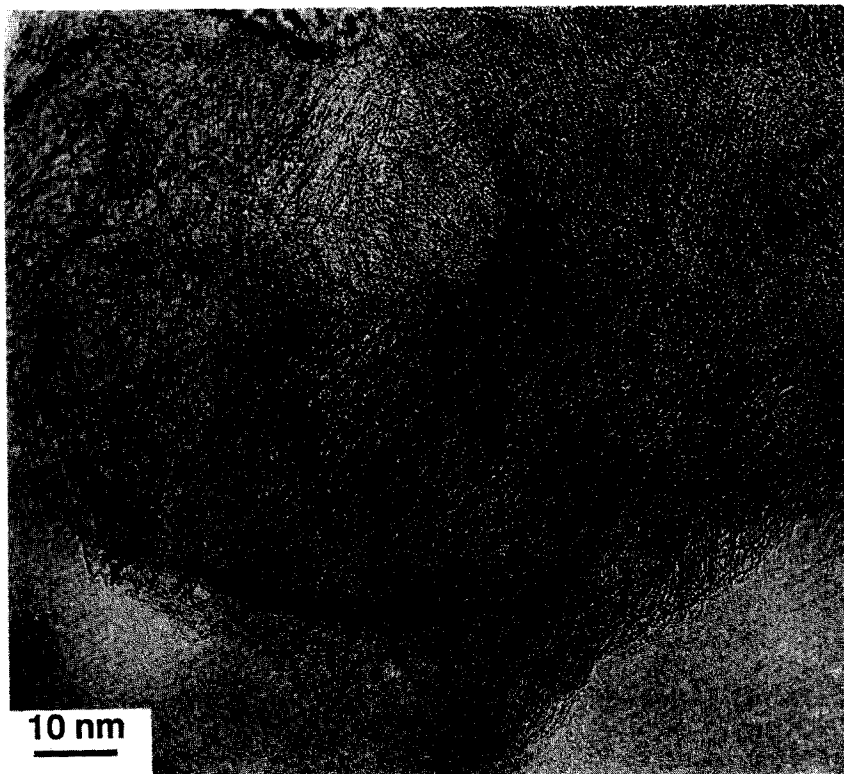
Another interesting kind of structure appears in the HF samples. They are shown in Fig. 10 and consist of tubules often presented in pairs, which do not contain a screw axis as do those reported by Iijima[4]. Both tubules in the pair have a growth that can be seen as a graphene sheet folded 360°. This kind of growth was pointed out and explained by Ugarte[15], who recognized that the bending of graphene basal planes eliminates the dangling bonds. In the (1010) surfaces, the energy of these structures is minimized (tube marked with A in Fig. 10). The tube marked with B has an irregular structure in the central part of the tube. Quite often, the tip of the tubules can have a faceted structure instead of being rounded.

### 3.3 Carbon fibers and nanotubes

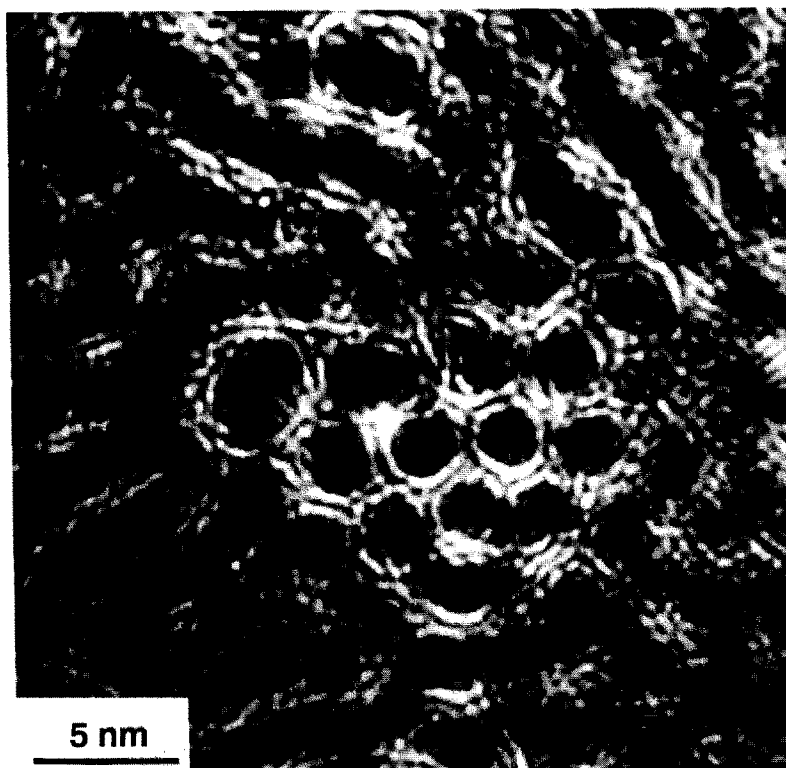
Carbon nanotubes can be produced with catalytic methods; however, at some critical point the growth

of the nanotube is stopped and pyrolytic carbon material begins to nucleate around the tube. Therefore, the carbon fibers produced in this way consist of a graphite tubular core surrounded by an amorphous material. A typical fiber obtained by this method is shown in Fig. 11. In this figure two fibers grow interconnected. There are some earlier works devoted to study the catalytic growth[16,17], and Endo[10] has proposed that there are two mechanisms for the growth of these fibers, the spiral growth model and the model of growth over impurity substrate particles. In the first model we expect to produce fibers of the type described by Iijima[4], which contain a screw axis along the growth directions. This could be the typical case of tubules grown up with the arc discharge method. However, in the catalytic method fibers do not necessarily contain a screw axis. Therefore, they correspond to tubules in a more general sense[18]. We have confirmed with electron diffraction of these fibers that in some cases a spiral axis is absent in CT samples.

An example of the initial states of the growth of a fiber around an Fe impurity particle is shown in Fig. 12a. The particle corresponds to  $\text{Fe}_3\text{C}$  (002) atomic planes with a distance between planes of 1.43 Å, as can be observed from the figure. Figure 12b shows an enlarged portion of the square marked in Fig. 12a. Here, the first layer of graphene wraps around the surface of the carbide. The rest of the



(a)



(b)

Fig. 6. Image of an array of ellipsoidal graphite rings. These can be self-organized in a lattice: (a) original image; (b) computer processed image to filter the noise.

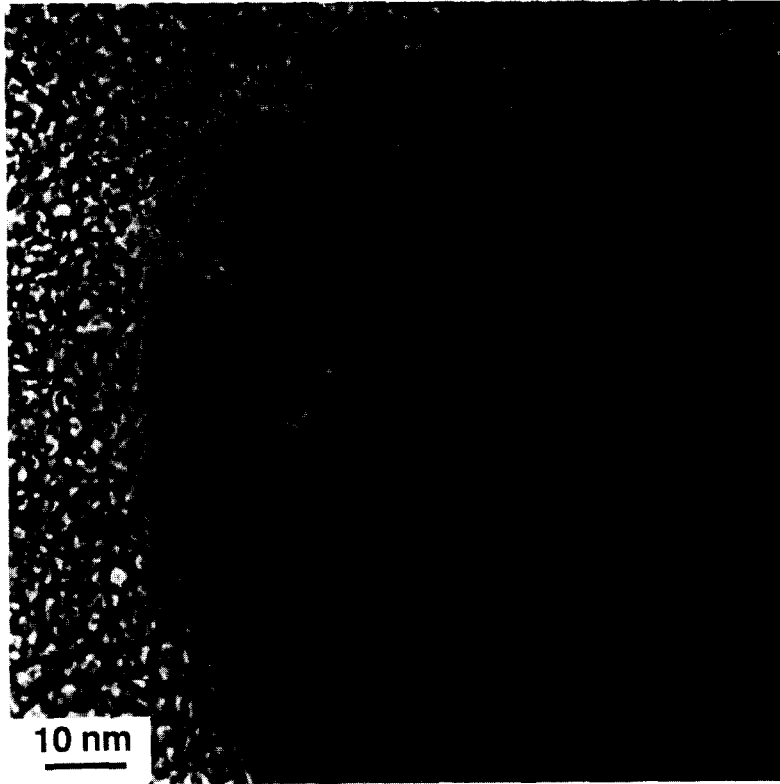


Fig. 7. Tangled graphene structures.

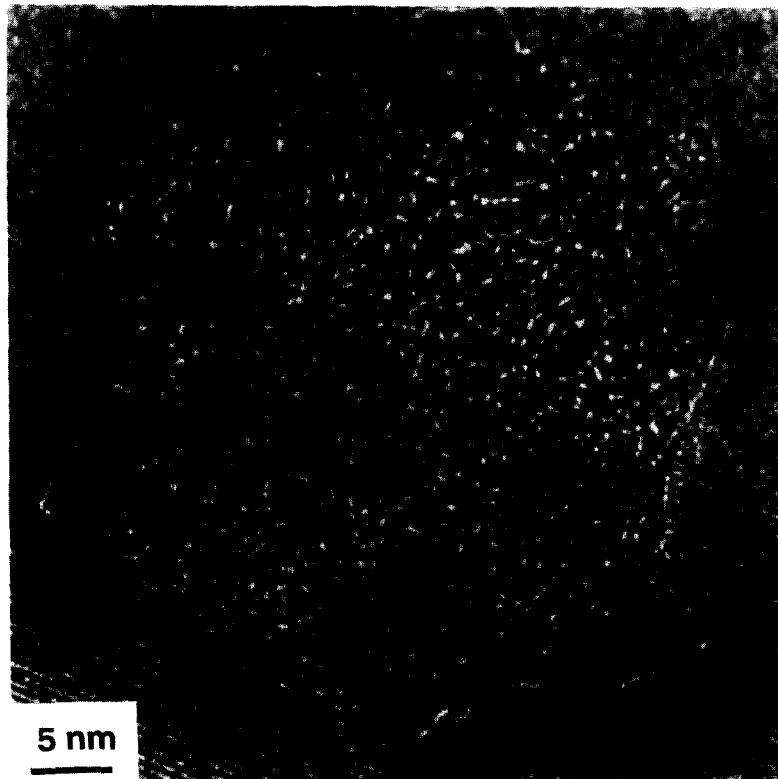


Fig. 8. Tangled ball of carbon attached to a nanotube.

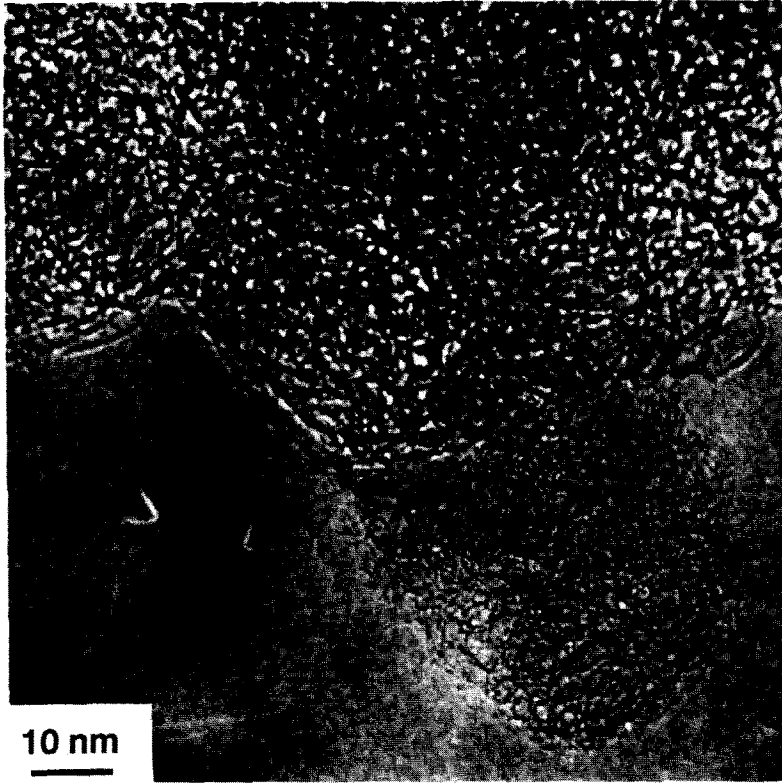


Fig. 9. Ball structure of a diameter of around 40 nm.

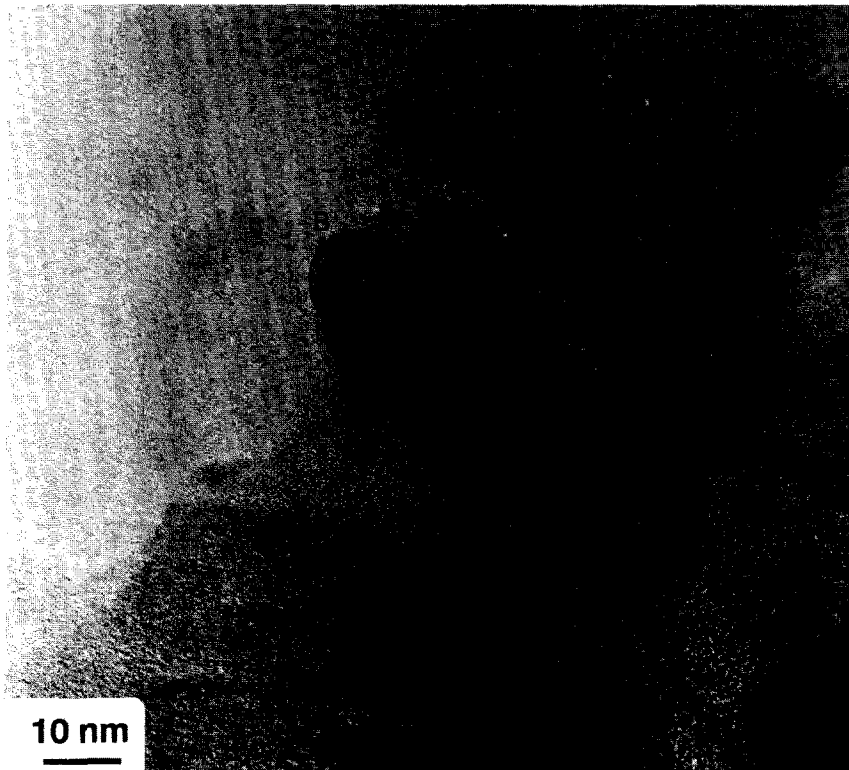


Fig. 10. A structure of two parallel tubes.

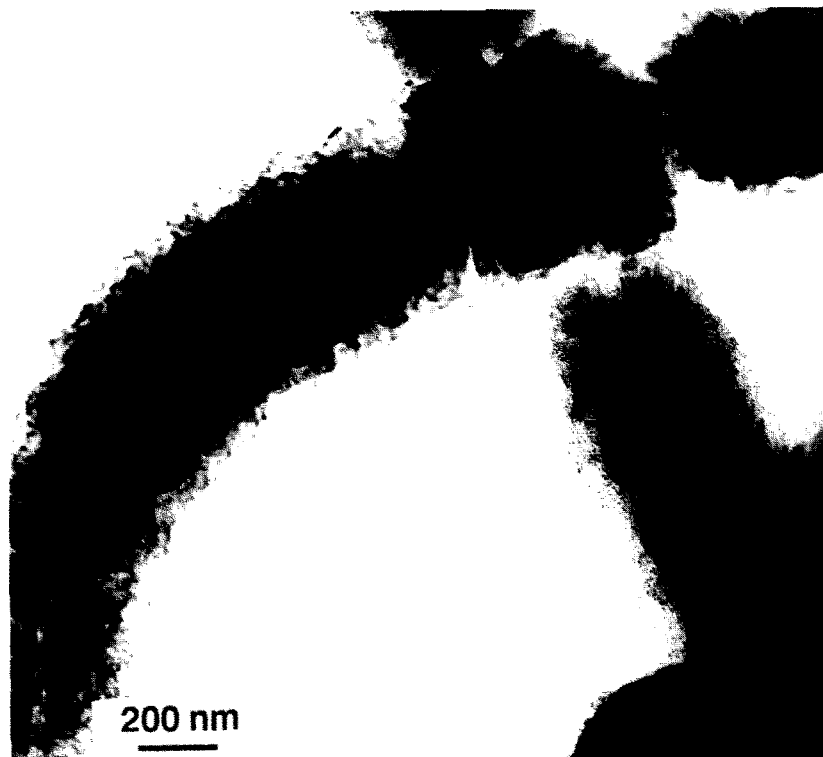


Fig. 11. Carbon fibers grown by a catalytic method. Note that the center of the fiber is a nanotube.

graphene layers start to grow up with the regular spacing of graphite  $3.35_4 \text{ \AA}$ . The tip structure might become faceted during the growth process, in a way similar to that described by Kato *et al.*[19].

As expected, the growth of these fibers adopts the shape of the metal particle over which it grows. Figure 13a shows a spherical particle around which a spherical array of graphene layers is nucleated. On the other hand, Fig. 13b shows an elliptical particle around which an elliptical structure of graphene is nucleated too.

Another set of fibers corresponds to pure graphene layers with no tubular structure. These graphitic fibers can grow to a considerable size, an example of that is shown in Fig. 14. Here, it is possible to observe some strain in the planes of graphite.

### 3.4 Small particles

When carbon soot is heated at 1003 K during 45 minutes, small carbon particles start to form. As we reported before[20], there are three basic types of particles: decahedral, icosahedral, and single twinned. An example of a decahedral particle is shown in Fig. 15. We have shown using EELS, that the particles correspond to carbon[20]. The spectra did not correspond to any of those reported in the literature for graphite, diamond, or amorphous carbon. However, the spectrum is closer to graphite than to the other structures. Electron diffraction

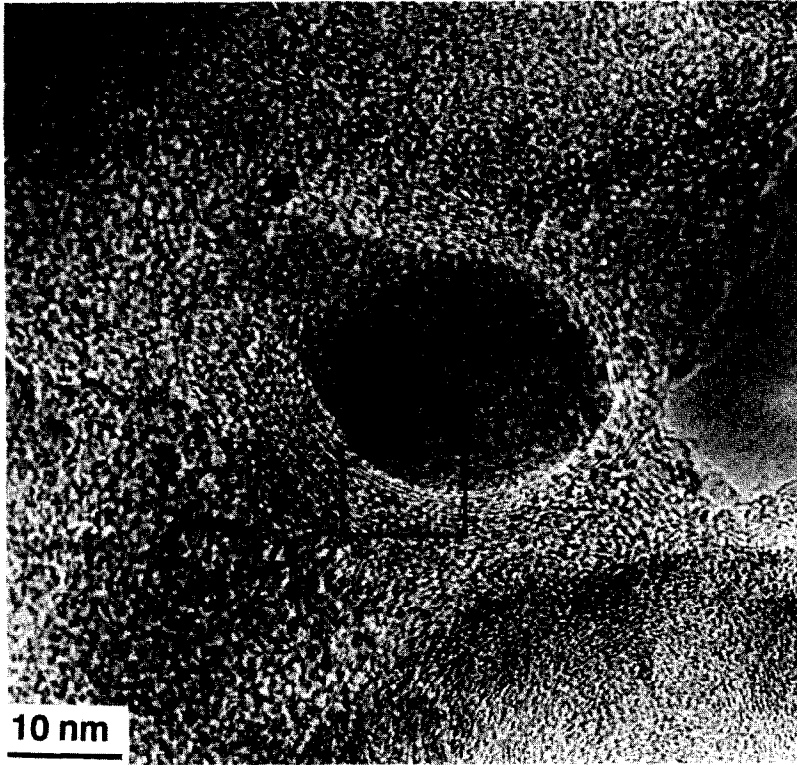
indicated a graphitelike structure[20]. The shape of the decahedral particle presented in Fig. 15 is peculiar, since one of the tetrahedral units of the decahedron has changed its shape. These kinds of changes in shape can be explained using a modified Wulff construction[19], which takes into account the twin boundary energy.

The asymmetric twin boundary observed in the decahedral particle will imply that the ratio of surface energy  $\gamma(111)/\gamma(100)$  is greater than  $3/2$ , if a basic cubic structure in the units of the decahedral particle is assumed.

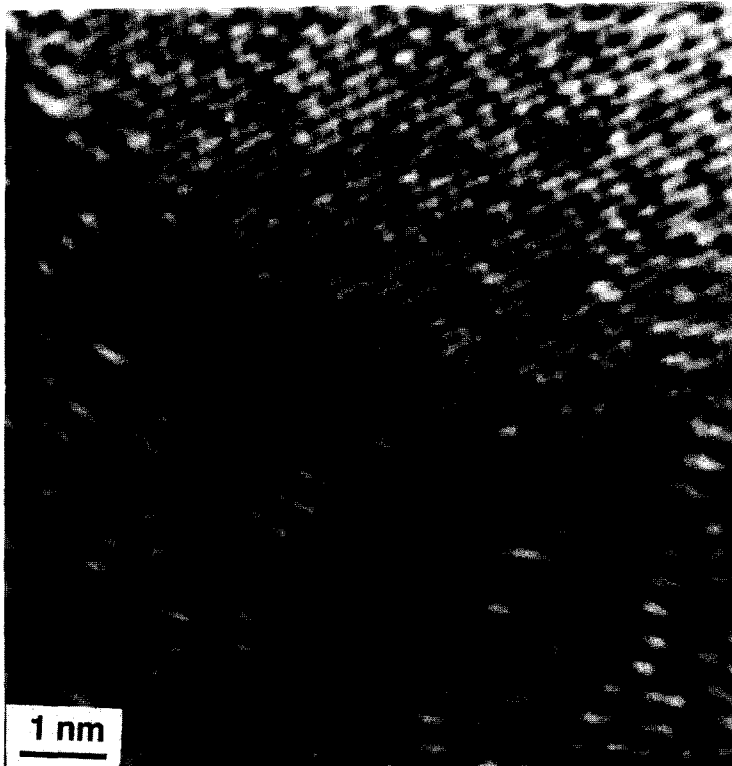
## 4. DISCUSSION

In the present work, we have shown several structures that can be grown with carbon. We have shown that carbon tends to form curved structures. Particularly interesting is the tangled structure shown in Figs. 8 and 9. Those figures show how flexible the graphene layers can be. This implies not only the existence of distorted trigonal bonds, but also of pentagonal and heptagonal arrays of carbon atoms. Tangled structures of carbon are not possible with standard graphite structure. Tangled structures offer very interesting possibilities for producing materials with a large surface area.

It is interesting to note that tangled structures become attached to the nanotubes. Moreover, the common observation is that these tangled structures

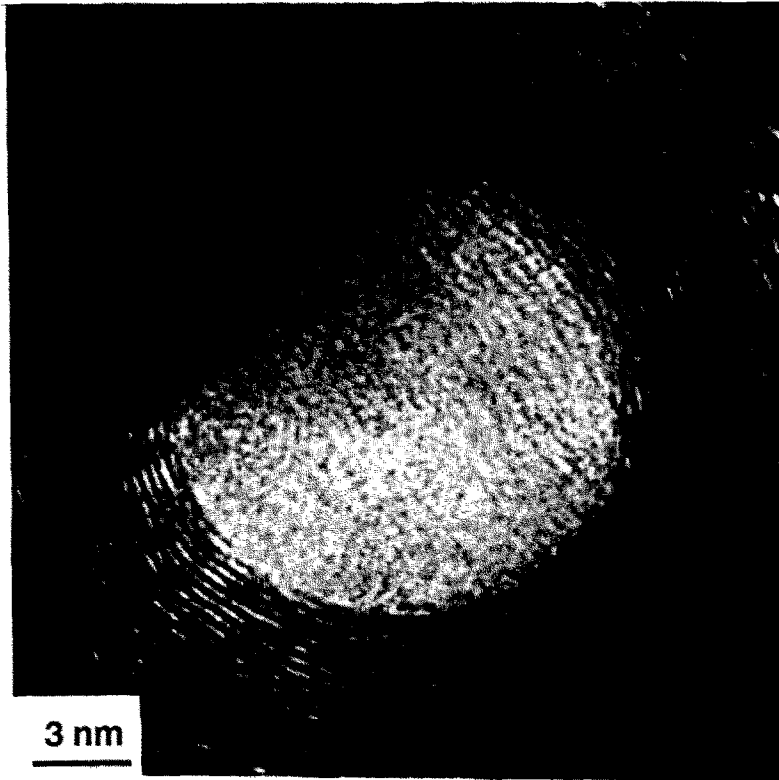


(a)

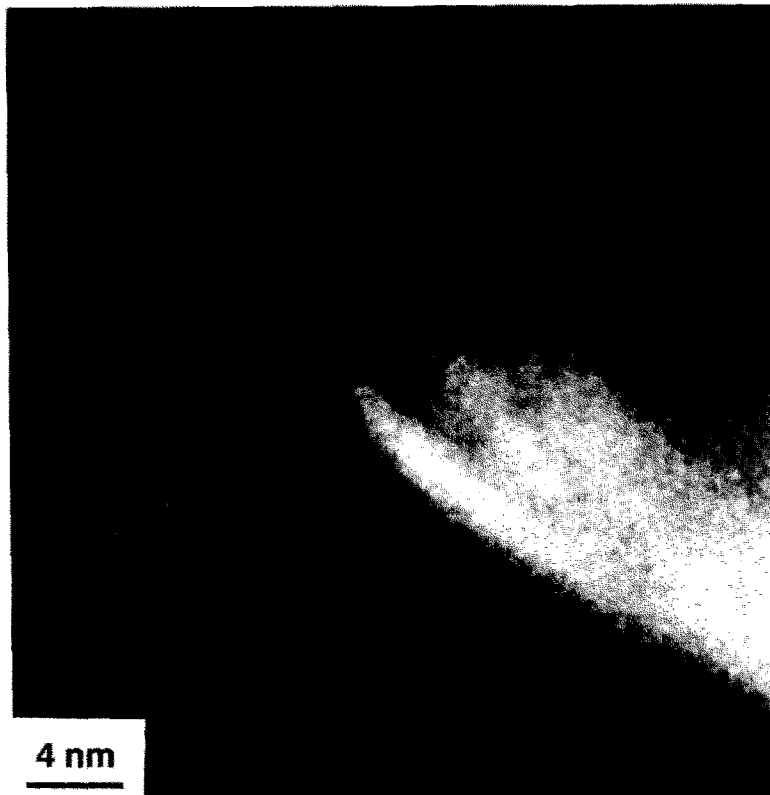


(b)

Fig. 12. Image of an  $\text{Fe}_3\text{C}$  particle, which is a nucleation center for growth of a fiber: (a) overall view; (b) a magnification of the marked area.



(a)



(b)

Fig. 13. Graphene layers, which grow around a particle following its shape: (a) spherical shape; (b) elliptical shape.

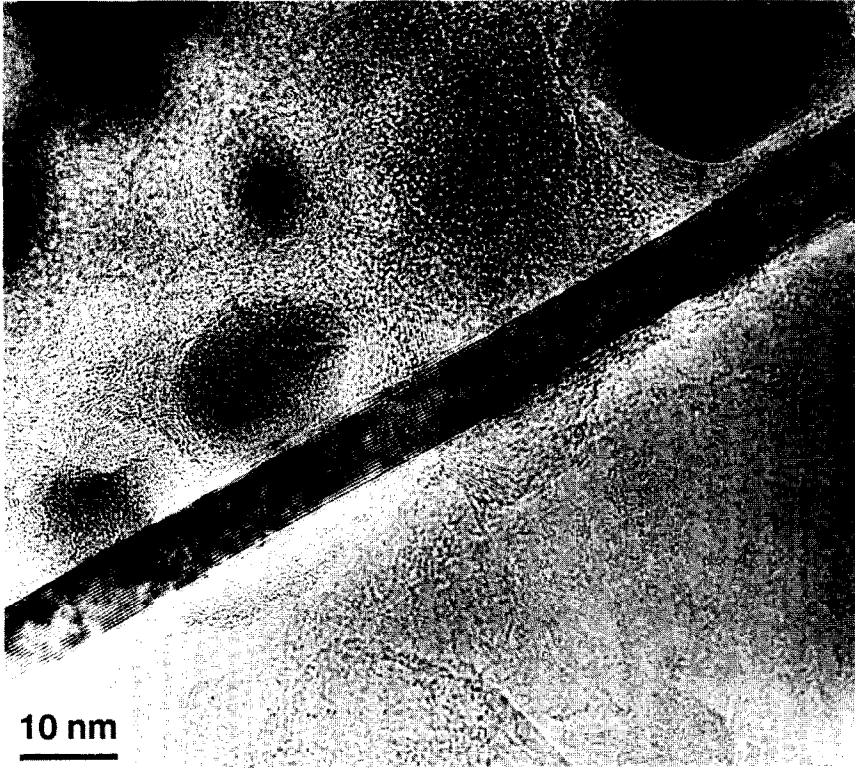


Fig. 14. Graphitic fibers without hollow center.

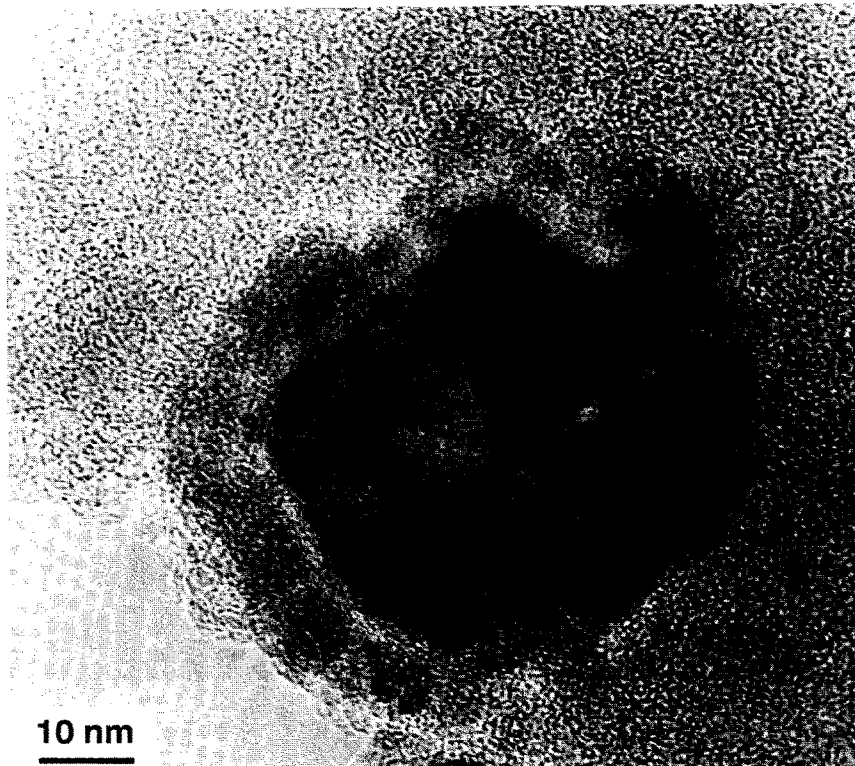
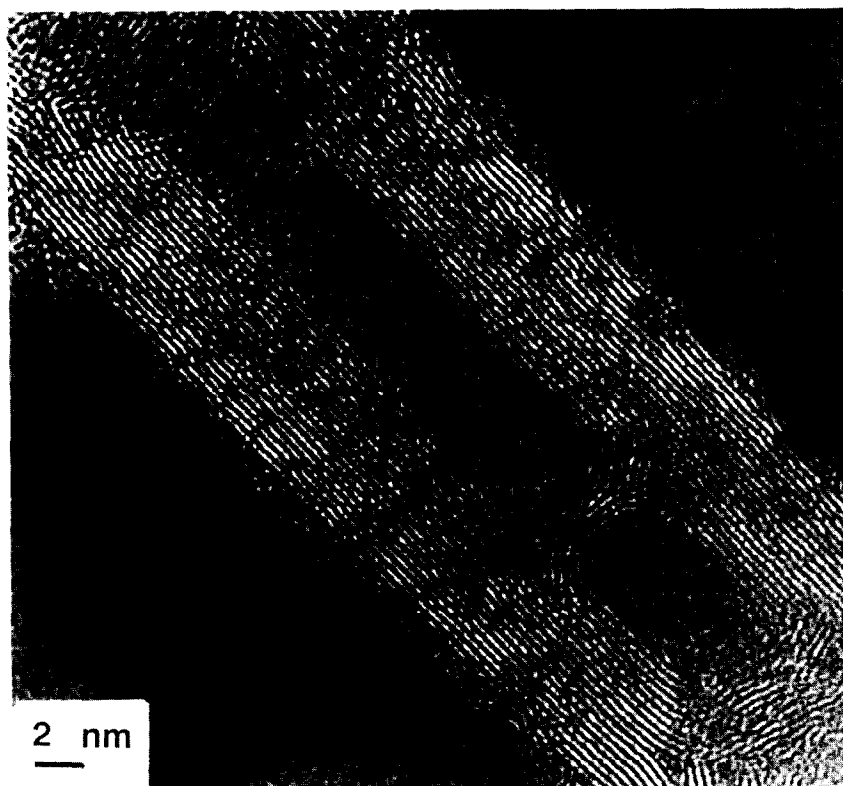
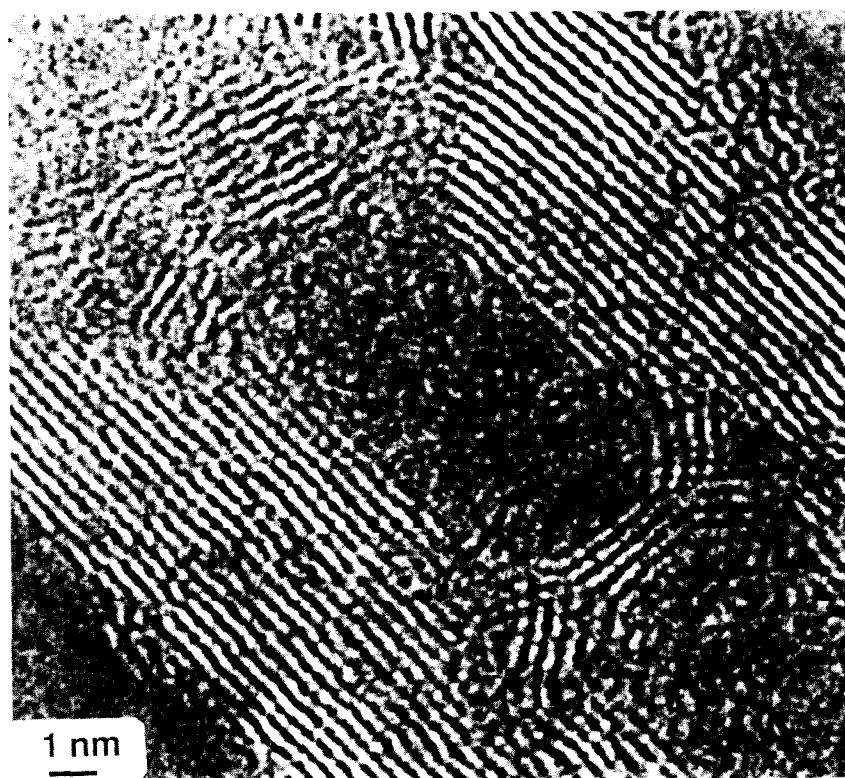


Fig. 15. Small particle of carbon with decahedral shape.

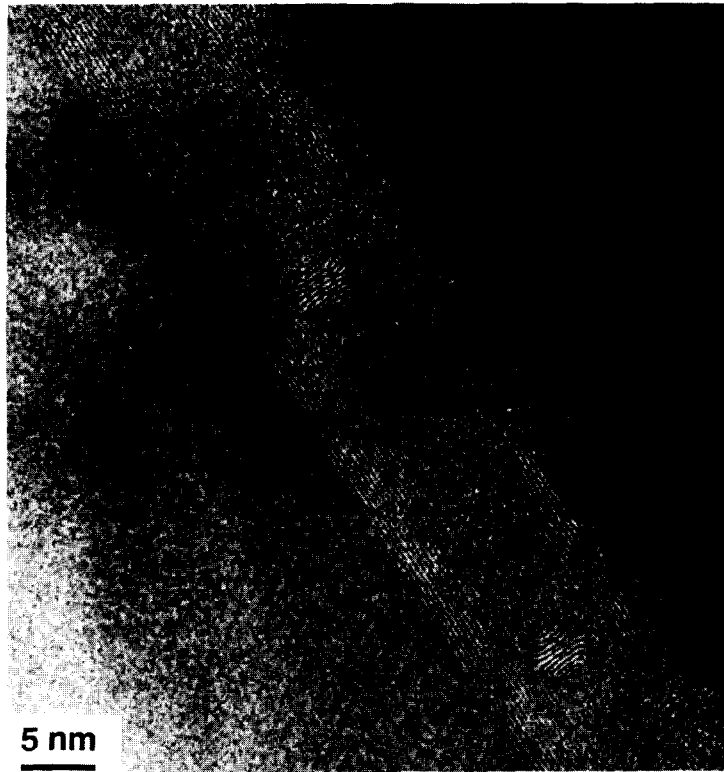


(a)

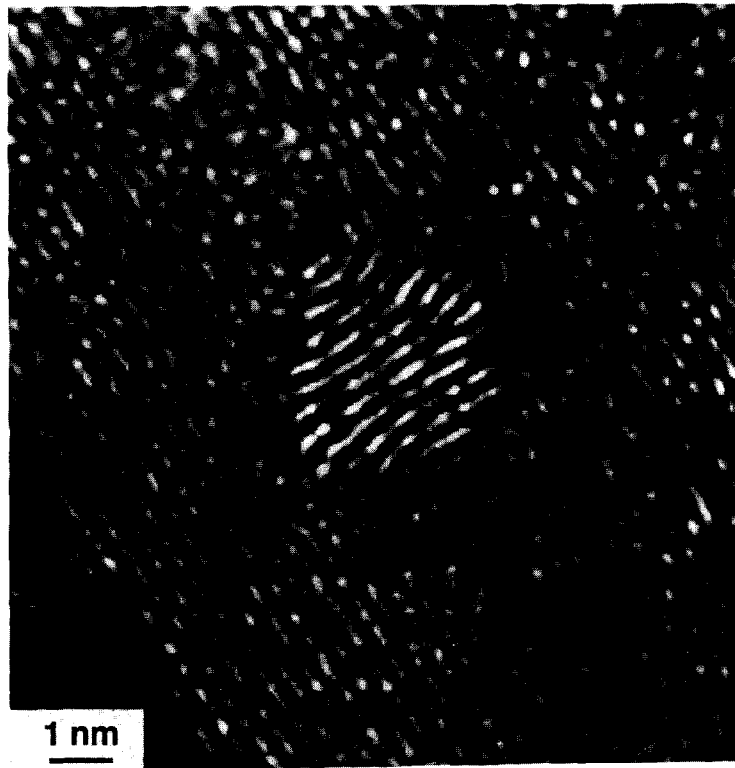


(b)

Fig. 16. (a) HREM image of a nanotube which shows a inner structure with faceting; (b) enlargement of image (a). These images have been computer processed.



(a)



(b)

Fig. 17. (a) Image of a nanotube with the center almost filled; (b) Enlarged image of the tube. These images were computer processed.

appear in groups, rather than as individual entities. This suggests that these structures may have many kinks and probably preferred absorption sites. This property could have some potential significance in catalysis.

The fact that carbon onion structures can be strongly faceted, as well as rounded, suggests that minimization of surface free energy should play a significant role in determining the final shape of the giant fullene structures. According to Ugarte[3], the onion structures become more ordered after electron irradiation. This was not observed by us. On the contrary, our structures become disordered after electron irradiation. It seems to us, that many of the onion structures observed are produced during the growth process. Our results are consistent with the findings of Dravid *et al.*[21]. These authors reported that the onion structures (bucky footballs in their terminology) are found in the fresh samples prior to electron beam irradiation.

In many cases, the onion structures are best described as conical structures, as discussed by Saito *et al.*[22]. We have also studied very carefully the interring distance in the onion structures. We have found that, in a systematic way, this distance is a few percent longer than in graphite. This was confirmed with electron diffraction on our samples. This finding agrees with the work of Saito *et al.*[22].

In a recent theoretical work Charlier and Michenaud[23] have discussed the energetics of nested multilayered systems composed of two infinite carbon tubules. In such a system, the energy gained by adding a new cylindrical layer around a central one was estimated to be 80% of the graphite dilayer binding energy. The calculated intertube distance was 3.39 Å, which is somewhat larger than that for the case of graphite. The structure shown in Fig. 4 is the smallest onion structure reported in the literature. This contains only four layers, so it becomes an ideal case to test the theory. We have accurately measured the interring distance for the onion of Fig. 4, using fast fourier transform techniques. These distances were compared with those of flat graphite in the same sample in a region close to that of interest given in Fig. 4. The result is that the interring distance is  $3.42 \pm 0.01$  Å, which is larger than in graphite. This is in agreement with the calculation of reference[23].

In the case of the graphite structures grown up from the vapor phase (CT samples), it is clear that the shape of the catalytic particle (Fe in the present case) is very important in determining the final shape of the structure. Two main classes of graphene structures were observed: pure graphitic fibers and hollow amorphous carbon fibers.

The first kind of structure can grow up to a very large size, and contains many defects, such as disclinations or internal strains. The second kind of structure contains nanotubes around its core. It seems to us, that in the first stages of growth, Iijima

nanotubes are produced. However, their growth stops after some layers, and an pyrolytic carbon structure begins to be formed. These structures can grow up to a size of the order of microns, and they have a graphene core.

It was pointed out by Dravid *et al.*[21] that an inner tube can grow up inside tubules. Examples are shown in Figs. 16 and 17 for AD samples. Here, two nanotubes with inner structures are shown. The images have been computer processed to increase contrast and to reduce noise. Figures 16a and 16b show that faceted structures with octagonal profiles are produced in the inner part of the main tube. In the case of Figs. 17a and 17b, the inner structure has grown until the tube is filled with carbon layers. In doing so, distorted atom planes are left inside the tube, as shown in Fig. 17b.

It has been suggested by Dravid *et al.*[21] that, the nanotubes sometimes can be fractured, and the resulting fragments eventually form closed shell fullerenes. This assumption relies on the frequent observation of bent tubes. We have some evidence in favor of this mechanism. In Fig. 5, a bent tube produces on its elbow a structure that is very close to an onion structure. Therefore, it is possible that, when the elbow is broken and goes apart from the rest of the tube, this new structure may grow up to become an onion structure. This follows the growth method proposed by Dravid *et al.*[21].

*Acknowledgments*—The authors are in debt to C. Zorrilla and L. Beltran del Rio for their technical support. We also acknowledge the CONACYT grant to support a postdoctoral stay (MMY) and the partial support of DGAPA-UNAM grant IN104493.

## REFERENCES

1. H. W. Kroto, J. R. Heath, S. C. O'Brien, R. F. Curl, and R. E. Smalley. *Nature* **318**, 162 (1985).
2. W. Krästchmer, L. Lamb, K. Fostiropoulos, D. Huffman, *Nature* **347**, 354 (1990).
3. D. Ugarte, *Nature* **359**, 670 (1992).
4. S. Iijima, *Nature* **354**, 56 (1991).
5. R. Tenne, L. Margulis, M. Genut, and G. Hodes, *Nature* **360**, 444 (1992).
6. M. Pederson and J. Broughton, *Phys. Rev. Lett.* **69**, 2689 (1992).
7. N. Hamada, S. Sawada, and A. Oshiyama. *Phys. Rev. Lett.* **68**, 1579 (1992).
8. R. E. Haufler *et al.* *J. Phys. Chem.* **94**, 8634 (1990).
9. M. José-Yacamán, M. Miki-Yoshida, S. Tehuacanero, and J. Santiesteban. *Appl. Phys. Lett.* **62**, 202 (1993).
10. M. Endo. *Chem. Tech.* **18**, 568 (1988).
11. M. Miki-Yoshida, L. Rendón, and M. José-Yacamán. *Carbon* (1993). In press.
12. S. Iijima, *J. Cryst. Growth* **50**, 675 (1980).
13. S. Iijima, N. Ajayan, and T. Ichihashi. *Phys. Rev. Lett.* **69**, 3100 (1992).
14. A. Mackay and H. Terrones, *Nature* **355**, 762 (1991).
15. D. Ugarte. *Chem. Phys. Lett.* **198**, 596 (1992).
16. M. Audier, A. Oberlin, M. Coulon, and L. Bonnetain. *Carbon* **18**, 73 (1980).

17. M. Audier, A. Oberlin, and M. Coulson. *J. Cryst. Growth* **55**, 549 (1981).
18. M. S. Dresselhaus, G. Dresselhaus, and R. Saito. *Phys. Rev. B* **45**, 6234 (1992).
19. T. Kato, K. Haruta, K. Kusakabe, and S. Morooka. *Carbon* **30**, 989 (1992).
20. M. Miki-Yoshida, L. Rendón, S. Tehuacanero, and M. José-Yacamán. *Surface Sci.* **284**, 3, L444 (1993).
21. V. P. Dravid, X. Lin, Y. Wang, X. K. Wang, A. Yee, J. B. Ketterson, and R. P. H. Chang. *Science* **259**, 1601 (1993).
22. Y. Saito, T. Yoshikawa, M. Inagaki, M. Tomita, and T. Hayashi. *Chem. Physics. Lett.* **204**, 277 (1993).
23. J. C. Charlier and J. P. Michenaud. *Phys. Rev. Lett.* **70**, 1858 (1993).